

# Use of Wind-Shear Displays for Doppler Radar Data



D. Chapman and K. A. Browning

Joint Centre for Mesoscale Meteorology, Department of Meteorology,  
University of Reading, Reading, United Kingdom

## ABSTRACT

The usefulness of displaying vertical wind shear on a radar range height indicator is demonstrated. Fine structure in the pattern of shear is shown to be helpful for inferring general flow patterns and the occurrence of billows due to shearing (Kelvin–Helmholtz) instability.

## 1. Introduction

Range height indicators (RHIs) of Doppler radar data are usually visualized using color shading to represent velocity. Although in general this clearly shows extrema in the data, it is very difficult to judge the magnitude of the velocity gradient in either the horizontal or the vertical, and it is even harder to tell if there is a pattern in this gradient field. In this paper we show that, when combined with the original Doppler velocity field, RHIs showing the vertical derivative of the Doppler velocity reveal patterns indicative of dynamical processes that would otherwise remain hidden.

Horizontal derivatives giving, for example, horizontal deformation and divergence, are occasionally displayed in the form of vertical cross sections and time–height plots of Doppler radar data. However, there have been few publications showing RHIs of the vertical derivative of the Doppler velocity (vertical shear). The few known to the authors have all been related to observations of Kelvin–Helmholtz (KH) billows. Starr and Browning (1972) showed the nu-

merical values of the vertical shear calculated over height increments of 200 m within billows that had a crest–trough amplitude of around 600 m. Browning et al. (1973a) showed the vertical shear calculated over height increments of 100 m through billows that had a crest–trough amplitude of between 230 and 450 m. Although both these studies showed that the shear had maxima in the billows themselves, the resolution of the measurements (compared to the amplitude of the billows) was insufficient to resolve details in the patterns of shear. Recently Chapman and Browning (1997) showed the shear calculated over height increments much smaller than the amplitude of the billows through which the measurements were made. These shear RHIs, obtained within frontal precipitation, show cat’s-eye and braided patterns that are very similar to the clear-air reflectivity “signatures” of KH billows (see, e.g., the review by Gossard 1990).

James and Browning (1981) showed time–height sections of vertical shear, calculated from high-resolution radar observations made at a fixed elevation angle of  $60^\circ$ , through the upper half of a train of billows. Although in retrospect the patterns seen by Chapman and Browning (1997) can be seen in their data, at the time the structures were not noted, perhaps because observations were not available over the whole depth of the billows. Brown and Rogers (1997) noted multiple shear layers in wind profiler data, possibly associated with gravity waves. However, the resolution of wind profiler data is insufficient to re-

---

*Corresponding author address:* Prof. Keith A. Browning, Joint Centre for Mesoscale Meteorology, Department of Meteorology, University of Reading, Whiteknights Rd., P.O. Box 243, Reading, Berkshire, RG6 6BB, United Kingdom.

E-mail: k.a.browning@reading.ac.uk

In final form 14 August 1998.

©1998 American Meteorological Society

solve structure due to KH billows, which is the main subject of this paper.

The data that we have examined have all come from the 3-GHz multiparameter radar (Goddard et al. 1994) at Chilbolton (51.15°N, 1.44°W), which is approximately 80 km north of the south coast of England. It has a range resolution of 300 m and an angular resolution of 0.28°. Although the angular resolution of this radar is unusually high, the success of the method we have used to identify patterns in the wind shear does not depend upon this. In fact, some of our results (not shown here) come from data at ranges of over 100 km, where the resolution is effectively similar to that which would be obtained from a lower-resolution radar at smaller ranges.

When the radar scans with a zero elevation angle, the Doppler velocity gives the horizontal component of the wind resolved along the azimuth of the radar beam. As the elevation angle increases, the radar detects a decreasing component of the horizontal velocity and this horizontal component is contaminated by the vertical fall speed of the targets (rain or snow in the studies presented here). However, for small elevation angles (less than around 10°) these errors in the measurement of the radial component of the horizontal wind are small enough to be neglected. In fact, if one is interested in the detection of essentially qualitative patterns in the data, they may be neglected even at elevations much greater than 10°.

The term “vertical shear” as used in this paper refers to the vertical derivative of the Doppler velocity, evaluated at constant range. Thus the component of vertical shear in the plane of the RHI, as shown in the figures in this paper, is given by

$$S_{i,j} = \frac{\partial V}{\partial Z} \approx \frac{V_{i,j+1} - V_{i,j-1}}{Z_{i,j+1} - Z_{i,j-1}},$$

where  $V$  is the Doppler velocity,  $Z$  is the height of the scanned volume, and the subscripts  $i$  and  $j$  refer to slant range and elevation angle, respectively. For observations made using the Chilbolton radar with an angular resolution of 0.28°,  $S$  is evaluated over a vertical distance given by  $\Delta Z \approx 10 \times \text{Range}$ , where the height and range are measured in meters and kilometers, respectively. The resulting shear has been smoothed to a small degree using a nine-point moving average around each point. This has been used here to reduce the effect of noise that is amplified when derivatives are calculated, although generally this was not found

to be a problem. There is a small error in the expression for  $S$  because for nonzero elevations it includes a component of the horizontal gradient of  $V$ . This error could be eliminated, although it would result in a more complex expression for the difference approximation. Since this error is appreciable only at large elevations we have neglected it in this study.

The following sections describe cases in which RHIs showing the vertical shear indicate the following:

- streamlines in approximately two-dimensional flow;
- KH billows signature, which in turn indicates mixing (and also possibly significant turbulence); and
- multiple shear layers associated with frontal zones.

## 2. Transverse circulation at a cold front

### a. Validation of streamlines

Figure 1a shows a Doppler velocity RHI (i.e., a vertical cross section) perpendicular to a rather two-dimensional cold front in which near-vertical line convection occurred at the surface front (at range 20 km). The front itself was orientated due south–north and moved eastward at around 15 m s<sup>-1</sup>. This front and its environment has been described by Browning et al. (1997), who derived front-relative streamlines, defined (assuming two-dimensional flow, with no divergence into the plane) by

$$\frac{\partial \psi}{\partial z} = \rho u,$$

with the boundary condition  $\psi = 0$  at the ground. However, here we have derived the streamlines in Fig. 1a instead by integrating downward assuming essentially horizontal flow above the front at 6 km. The streamfunction is zero on this upper boundary, which was chosen to be sufficiently high that it was above the regions of significant vertical velocity, yet low enough to have only a small region below it in which data were not available. Velocities in this region were reconstructed using averages of the surrounding values. Integrating downward from an upper boundary in this way slightly reduces the problems of error growth associated with the decrease in density with height when integrating upward. The resulting streamlines in Fig. 1a indicate that cold air approached the surface front from the west, then ascended and receded to the

west. Warm air approached the front from the east, rose at the surface front, then continued to flow to the west, ascending gently over the cold air.

In Fig. 1b we use the pattern of vertical wind shear as a guide to validate the independently derived streamline pattern. The justification for being able to do this is as follows. For two-dimensional, inviscid, irrotational flow in which the background density remains constant with height, the component of vorticity lying in a vertical plane (i.e.,  $\eta = \partial w/\partial x - \partial u/\partial z$ ) is conserved following the flow. This is as a result of there being no stretching or compression of vortex tubes into the plane. Thus, for steady flow, contours of the component of vorticity lying in the plane would indicate the orientation of streamlines, as flow would be along contours of the vorticity. In practice, a layer of enhanced vorticity, which will also indicate the orientation of streamlines even if the background density varies with height, will be easier to identify and follow if shading is used to represent the vorticity. For most parts of the flow, except near the line convection and where the cold air reverses direction,  $\partial w/\partial x$  is considerably smaller than  $\partial u/\partial z$ , so the orientation of a layer of vertical shear on its own will give a good indication of the orientation of the streamlines. The main reason for nonconservation of vorticity in two-dimensional flow is likely to be dissipation, especially in any strong shear layer. However, to a first approximation the dissipation will simply spread the shear in the vertical, so it will still be appropriate to use the layer to indicate a streamline, so long as the flow is steady.

Figure 1b shows as shaded just the positive values of the vertical shear, with the streamlines superimposed. Although there was some deformation at the front, resulting in nonconservation of the component of vorticity in the plane, the near-zero values of vertical velocity at low levels (calculated from the streamfunction) implies that this was small. As a result, the diffuse shear layer that extends across the domain at a height of about 1 km ahead of the surface front and then rises by 20-km range to around 4 km behind the front is a good indicator of a streamline following air that rises just

above the frontal zone. There is good agreement between this shear layer and the previously derived streamlines that lie close to it, indicating that the assumptions used in the derivation of the streamlines were justified. Note that the region of strong easterly flow (dark shading in Fig. 1a) also follows the streamlines of the ascending flow, indicating approximate conservation of this component of momentum within the flow. In cases where appropriate boundary conditions cannot be imposed (perhaps due to lack of data near the ground), a shear layer as shown in Fig. 1b could be used to define a streamline, and the remaining streamlines could be obtained by integration away from it.

### b. Shear structures

Chapman and Browning (1997) showed that the shear within large-amplitude billows that were clearly visible in the Doppler returns from frontal precipitation had a cat's-eye structure that was similar to the clear-air reflectivity patterns observed by, for example, Browning (1971). Figure 1c shows similar patterns in the layer of negative shear at a height of 2 km between

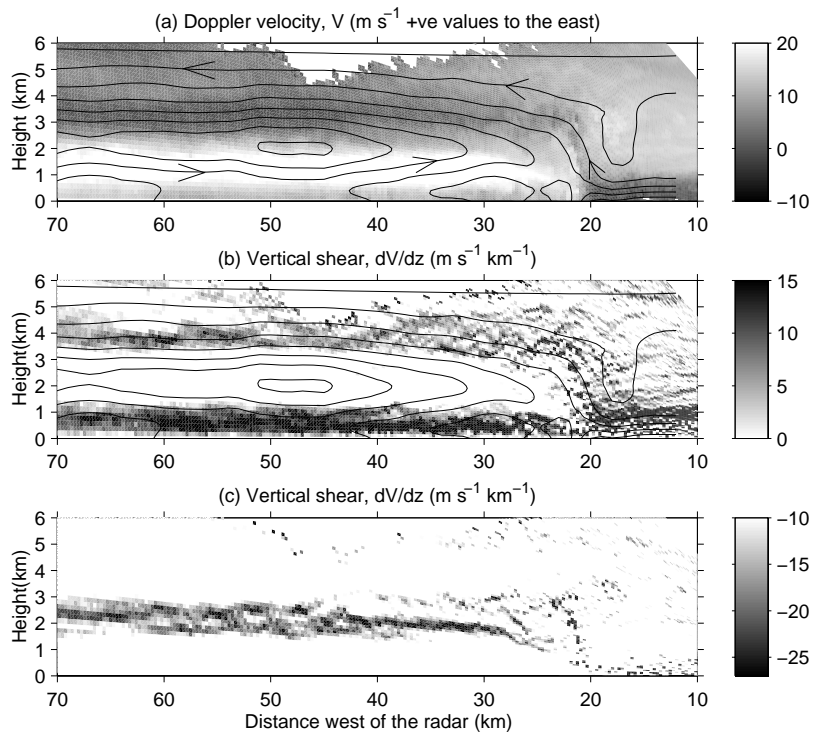


FIG. 1. Data from Chilbolton radar at 1844 UTC on 24 October 1995 at an azimuth of  $270^\circ$ . Note that west is to the left of these plots. (a) Doppler velocity,  $V$  ( $\text{m s}^{-1}$ ). (b) Positive values of vertical shear,  $\partial V/\partial z$  ( $\text{m s}^{-1} \text{ km}^{-1}$ ), as defined in the text. (c) Negative values of vertical shear. A mass-weighted streamfunction (intervals of  $4 \text{ kg m}^{-2} \text{ s}^{-1} \text{ km}$ ) derived from the Doppler velocity data has been used to overlay (a) and (b).

ranges 40 and 60 km. There are other very shallow layers of negative shear at other heights in Fig. 1c, especially between 10- and 40-km range, but we are concerned only with the more significant layer of negative shear that shows up boldly in Fig. 1c centered at a height of 2 km. The cat's-eye pattern at 40–60-km range could be clearly seen in a similar location relative to the front in a number of other RHIs at different times. It has a crest–trough amplitude of 1 km and a wavelength of around 4 km, so in these terms could be described as a train of large-amplitude billows. However, the intensity of the shear is sufficiently weak that the velocity perturbation is too small to be detected easily in the original Doppler field.

The most likely cause of the cat's-eye structure seems to be KH billows, although it could possibly be due to an interaction between one thin shear layer and a second such layer, just above. Assuming that the pattern in the shear layer is the result of KH billows, the location relative to the streamline pattern is such that they would have been mixing *within* the weakly stratified cold air mass rather than at its boundary. Thus the billows are unlikely to have had a significant effect on the thermodynamic structure of the front, although they would have affected the kinematic structure by redistributing the shear.

To the extent that the front is similar in structure to a density current, KH billows might have been expected close to the “head” between the cold and the warm airflows (i.e., between range 25 km, height 3 km and, say, range 50 km, height 5 km) as in Figs. 5 and 6 of Xu et al. (1996). However, the lack of any distinct cat's-eye structure in this region indicates that large-amplitude KH billows were *not* occurring here, so there was less large-scale mixing across this front than might be expected from a comparison with models of density currents.

### 3. Mixing within frontal zones

The main aim of the previous section was to show that features are clearly visible in RHIs showing the vertical shear but may be almost completely invisible in the original Doppler velocity RHI. This is particularly true for KH billows, which give rise

to a characteristic signature in the shear. The following sections use this property of the shear RHI to identify regions containing KH billows and mixing, primarily within sheared frontal zones.

#### a. Dual upper cold fronts

Figure 2a shows a Doppler RHI through a pair of upper cold fronts that overran a surface warm front on 5 January 1998. Each upper cold front has a thermally direct circulation associated with it, as indicated by the arrows in the figure. The structure is similar to that described by Browning et al. (1973b) (see Fig. 8 of their paper for a schematic diagram of the processes occurring).

Again the Doppler velocity field is smooth, which would seem to imply that strong mixing is not occurring between the cold and warm air. However, close inspection of the data between ranges 45 and 55 km at a height of around 3 km does show some weak wavelike perturbations to the velocity field. These perturbations are much clearer in the shear RHI in Fig. 2b and appear as braids/cat's-eye structures, indicating the existence of KH billows inducing mixing over a depth of 1 km at the statically stable interface between the descending cold and dry upper-tropospheric air and the ascending warm and saturated lower-tropospheric air. Similar structures existed for the next 30 min, until this region had moved too far away from the radar for them to be resolvable. Four separate frontal circulations were sampled by the radar during the observation time (two of which are visible in Fig. 2). Shear structures also existed in some

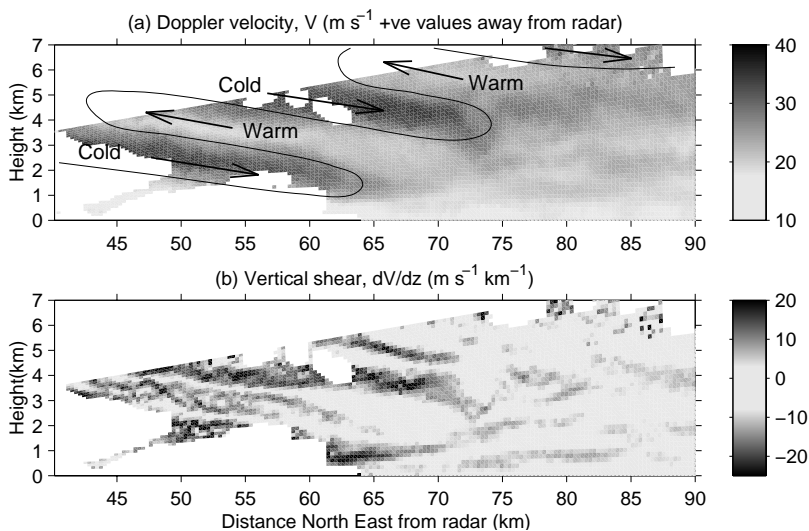


FIG. 2. Data from Chilbolton radar at 1118 UTC on 5 January 1998 at an azimuth of 47°. (a) Doppler velocity,  $V$  ( $\text{m s}^{-1}$ ). (b) Vertical shear,  $\partial V/\partial z$  ( $\text{m s}^{-1} \text{ km}^{-1}$ ).

of the other interfaces associated with these circulations, though they were less distinct, and data were not available in some regions because of evaporation of the precipitation as it fell through the cold, dry air.

While in the previous case (Fig. 1) mixing occurred primarily within the cold airflow, in this case mixing occurred across the strongly sheared boundary separating air with different thermodynamic properties and origins. This means that the induced mixing is likely to have been of more importance in terms of the effect on thermodynamic profiles. It is also of potential importance in bringing together different chemical species, which may then react influencing the distribution of chemicals in the upper troposphere.

*b. Mixing associated with fronts during FASTEX*

The Fronts and Atlantic Storm Track Experiment (FASTEX) (Joly et al. 1997) was carried out during January and February 1997. Intensive observations were made of storms and fronts as they developed over the Atlantic, some of which then moved over the United Kingdom. During this experiment, the Chilbolton radar was scanned frequently. The scans were made using automated scanning sequences, obtaining RHIs and plan position indicators (PPIs) alternately through the majority of precipitating frontal regions that passed over the radar between 4 and 25 February. This dataset is likely to give a good indication of the type and frequency of shear features occurring in frontal regions associated with cyclones over the United Kingdom during winter.

The data were studied by looking at both the original Doppler data (RHIs and PPIs) and RHIs of the vertical shear. The results are as follows (see Table 1).

- The vast majority of data were from the vicinity of

fronts, with a clearly defined vertical shear direction over the depth of the front. Those data (from only a few days) that did not show this have been disregarded in the following paragraphs, as their inclusion would only confuse the points made.

- The majority of the RHIs did not show a single vertical layer over which all the shear (and presumably stability) was concentrated. Instead they showed multiple shear layers on vertical scales of around 1 km.
- Although many of these shear layers remained “laminar” (to the resolution of the radar) for much of the observing time, in every observation period (normally lasting a few hours) there were some

TABLE 1. The occurrences of braids (Br) and cat’s-eyes (C-E) (as indicated in Fig. 3) within shear layers in the vertical derivative of Doppler data from Chilbolton radar during February 1997. The times relate to the period of observation, not to the duration of the features (most were only observed for a short time relative to the total observation period). The letters w, m, and s (weak, medium, and strong, respectively) refer to a subjective estimation of the strength/clarity of the relevant feature. The depth (in km) refers to the approximate vertical extent of the feature/shear layer. The synoptic situation relates to the time at which the “most interesting” features occurred. SCF and SWF refer to surface cold front and surface warm front, respectively.

Date	Obs. times	Br	C-E	Depth	Synoptic situation
4	1000–1023	–	–	–	Ahead of SCF, behind SWF
4	2300–2330	s	–	0.5	Above SCF
7	1050–1600	m	w	1.0	Just behind SCF
10	0800–1343	m	w	0.7	Ahead of SCF
11	1200–2010	s	s	1.0	Just ahead of SWF
11	2230–0154	–	–	–	Behind SWF
12	1750–2110	w	–	–	At/behind SCF
13	0030–0330	m	w	1.0	Behind SCF
14	0845–1349	m	–	0.4	Close to SWF and SCF
17	1830–2230	w	w	0.8	Behind SCF
19	1624–1727	w	–	1.0	At/behind SWF
21	0845–1015	m	–	0.4	Behind SCF/in front of SWF
24	1445–1840	s	m	1.0	Close to SWF and SCF
25	1640–1900	m	w	1.0	Behind SCF

RHIs in which the shear layers showed “structure” to some degree. This structure consisted of distinct shear patterns, which were coherent over a number of scanning volumes. (It has not been possible to estimate the duration of these features from the data available because the scanning sequences were such that billows would be missed on a large number of occasions, or observed for only part of the time during which they existed within range of the radar. Also, the radar scans were frequently made such that they scanned mainly perpendicular to frontal regions, rather than parallel to them, so they were not in the appropriate direction for detection of billows generated as a result of the thermal wind shear in a frontal zone.)

- The shear layers in which this structure was observed were classified according to Fig. 3. In addition, a subjective estimation of the strength and clarity of the structure was made. Under this scheme, the structures in Fig. 2, for example, would be classified as cat’s-eyes with medium strength/clarity. Table 1 shows that the braids and cat’s-eyes all had a vertical extent less than or equal to around 1 km. This is true of all observations of KH billows in the atmosphere known to the authors. Billows of 1 km vertical extent appear to be surprisingly abundant in the data compared with still-resolvable billows of, say, half this amplitude.
- The majority of occurrences of braids or billows occurred actually *within* frontal zones and were not merely loosely associated with them, as in the case shown in Fig. 1c.

Even though this study is preliminary, the results clearly show that frontal zones often contain multiple shear layers and that these shear layers frequently show evidence of mixing as a result of KH billows. This is in contrast with the way fronts tend to be represented in most numerical weather prediction models, in which a frontal zone will usually be shown as one shear layer over which, in some cases, mixing is not parameterized in the free atmosphere.

#### 4. Conclusions

This paper has demonstrated the utility of looking at RHIs of vertical shear in addition to RHIs of Doppler velocity, especially for the identification of



FIG. 3. Classification of the structures observed frequently within vertical shear RHIs. The lines show the patterns of maximum shear. Braids, cat’s-eyes and a turbulent layer are represented in (a)–(c), respectively.

regions containing KH billows. It appears that RHIs of the vertical shear may be used to detect KH billows in regions of precipitation in the same way that reflectivity from high-power radars has been used in the past to detect KH billows in the clear air. This ability to confidently infer the presence or absence of KH billows makes it possible, in principle, to obtain a climatology of billows in regions of precipitation as well as in the clear air.

From the results of the preliminary study presented here, it appears that KH billows occur considerably more often than might be inferred from inspection of Doppler velocity RHIs alone, even in cases where the billows are of large amplitude, up to 1 km in depth. Billows, and other less well-defined shear features presumably associated with billows, occur predominantly in frontal shear zones, where they may have a significant effect on the kinematic, thermodynamic, and chemical properties of the atmosphere. The method described here provides a way of estimating these effects, and whether or not they have significance for weather prediction.

*Acknowledgments.* We are grateful to the Radio Communications Research Unit at Rutherford Appleton Laboratory for access to the Chilbolton radar. Daniel Chapman is supported by a studentship from the Natural Environment Research Council.

#### References

Brown, W. O. J., and R. R. Rogers, 1997: Gravity wave and wind shear observations on the McGill weather and profiler radars. *Proc. 28th Conf. Radar Meteorology*, Austin, TX, Amer. Meteor. Soc., 512–513.

Browning, K. A., 1971: Structure of the atmosphere in the vicinity of large-amplitude Kelvin–Helmholtz billows. *Quart. J. Roy. Meteor. Soc.*, **97**, 283–299.

—, G. W. Bryant, J. R. Starr, and D. N. Axford, 1973a: Air motion within Kelvin–Helmholtz billows determined from simultaneous Doppler radar and aircraft measurements. *Quart. J. Roy. Meteor. Soc.*, **99**, 619–638.

—, M. E. Hardman, T. W. Harrold, and C. W. Pardoe, 1973b: The structure of rainbands within a mid-latitude depression. *Quart. J. Roy. Meteor. Soc.*, **99**, 215–231.

- , N. M. Roberts, and A. J. Illingworth, 1997: Mesoscale analysis of the activation of a cold front during cyclogenesis. *Quart. J. Roy. Meteor. Soc.*, **123**, 2349–2375.
- Chapman, D., and K. A. Browning, 1997: Radar observations of wind-shear splitting within evolving atmospheric Kelvin–Helmholtz billows. *Quart. J. Roy. Meteor. Soc.*, **123**, 1433–1439.
- Goddard, J. W. F., J. D. Eastment, and M. Thurai, 1994: The Chilbolton advanced meteorological radar: A tool for multi-disciplinary research. *Electr. Commun. Eng. J.*, **6**, 77–86.
- Gossard, E. E., 1990: Radar research on the atmospheric boundary layer. *Radar in Meteorology*, D. Atlas, Ed., Amer. Meteor. Soc., 477–527.
- James, P. K., and K. A. Browning, 1981: An observational study of primary and secondary billows in the free atmosphere. *Quart. J. Roy. Meteor. Soc.*, **107**, 351–365.
- Joly, A., and Coauthors, 1997: The fronts and Atlantic storm-track experiment (FASTEX): Scientific objectives and experimental design. *Bull. Amer. Meteor. Soc.*, **78**, 1917–1940.
- Starr, J. R., and K. A. Browning, 1972: Doppler radar measurements of clear air turbulence. *Proc. 15th Conf. Radar Meteorology*, Champaign-Urbana, IL, Amer. Meteor. Soc., 248–251.
- Xu, Q., M. Xue, and K. Droegemeier, 1996: Numerical simulations of density currents in sheared environments within a vertically confined channel. *J. Atmos. Sci.*, **53**, 770–786.

